Ground and First-Excited Global Potential Energy Surfaces of the H_2O^+–He Complex: Predictions of Ion Mobilities

XIN CHEN, M. THACHUK

Department of Chemistry, University of British Columbia, Vancouver V6T 1Z1, Canada

Received 1 December 2003; accepted 7 April 2004
Published online 25 August 2004 in Wiley InterScience (www.interscience.wiley.com).
DOI 10.1002/qua.20199

ABSTRACT: Ion mobilities of H_2O^+ drifting in helium are calculated and compared with experiment. These calculations employ global potential energy surfaces of the H_2O^+–He complex, which in the present case were calculated ab initio at the unrestricted MP2 level of theory using a basis set of aug-cc-pVTZ quality, and treating the ion as a rigid body. Details are presented of the general characteristics of both the ground and first-excited electronic states of the complex. Although only the ground-state surface was used for the mobility calculations, the ab initio determination of the ground state necessitated the inclusion of the first-excited state owing to the presence of a crossing between the two. This crossing is also described. Mobilities calculated from the global surfaces are in good agreement with experiment. Int J Quantum Chem 101: 1–7, 2005

Key words: H_2O^+–He complex; first-excited state; MP2; ion mobility; global energy surface

1. Introduction

Ion mobility experiments have been used for several decades to separate, isolate, and identify ions of different sizes and conformations. Recent experiments have studied large, biological ions such as proteins, amino acids, and oligonucleotides, from which some knowledge of different ion conformations can be reasoned [1–5]. Collision-induced rotational alignment has attracted experimental [6–10] and theoretical [11–17] interest. This alignment results when ions or molecules experience collisions preferentially in one direction, and is a function of their overall shape. Recent work in our group has looked at some of the microscopic details of this alignment mechanism [18–20].

A natural extension of these studies on linear ions is to consider planar, nonlinear ions. For this

Correspondence to: M. Thachuk; e-mail: thachuk@chem.ubc.ca
Contract grant sponsors: Natural Sciences and Engineering Research Council of Canada; Canada Foundation for Innovation.
This article contains supplementary material available via the Internet at http://www.interscience.wiley.com/jpages/0020-7608/suppmat.

reason, H_2O^+ drifting in helium was chosen as a candidate system. In this case, mobilities are calculated using a classical, molecular dynamics method that requires forces derived from global potential energy surfaces, extending from small to asymptotic radial distances. To date, one of the most comprehensive ab initio studies of H_2O^+–Rg complexes have been carried out by Dopfer and coworkers [21–24], who explored geometries at intermediate radial distances with C_s and C_{2v} symmetries. However, these geometries span only a small subset of the global potential energy surface needed for the scattering trajectories that determine ion mobilities. Hence, the present work reports on the determination of these surfaces at the unrestricted MP2 level of theory.

While the mobility calculations require only the ground-state potential surface, inclusion of the first excited state surface was necessitated by the discovery of a curve crossing at small radial distances. To resolve the states in this region, it was necessary to separate the contributions due to the ground state from those of the first-excited state. In the end, the global surface for the first excited state was also determined at the same level of theory. General characteristics of these two surfaces will be presented, along with some discussion of their crossing.

Section 2 will describe the methods used in calculating the potential energy surfaces, as well as the subsequent ion mobilities. Descriptions of the potential energy surfaces are given in Section 3, along with the prediction of the ion mobilities. Section 4 closes with a discussion.

2. Methods

The potential energy surfaces were calculated using Gaussian 98 [25]. Roth et al. [24] have explored the potential energy surface of the H_2O^+–He complex for a series of geometries of C_s and C_{2v} symmetry, that is, when helium is restricted to the plane of the H_2O^+ ion, and to a plane perpendicular. They employed an aug-cc-pVTZ# basis set [21] at the unrestricted MP2 level of theory to predict a variety of spectroscopic parameters successfully. The same level of theory was chosen for the present calculation, and the basis set used was identical to that of Roth et al. [24]. The final contraction of the basis is described by (11s7p3d2f) → [7s4p3d2f] for O and (6s3p2d) → [4s3p2d] for H and He. Further details of the basis set can be found in Ref. [21].

At small radial distances, a curve crossing exists for specific geometries of the system, and the default electronic configuration population algorithms in Gaussian fail to yield the ground-state surface in all cases. To resolve the two lowest energy states for all configurations, the following procedure was employed. First, preliminary single-point calculations were used to determine the ground-state orbital occupancies in different regions of configuration space, and occupancy changes needed to go from the ground to the first-excited state. It was found that in all cases, the lowest two energy states resulted from one of three possible orbital occupancies. To determine the global surfaces at all configurations, three separate calculations were performed, one for each possible orbital occupancy (which was specified manually in the Gaussian input file). For each case, an MP2 calculation was performed after the self-consistent field (SCF) orbital occupancies had been assigned, so that all the potential surfaces were calculated at the same level of theory.

After these triplets of energies were calculated at each point in configuration space, they were ordered from lowest to highest. The two lowest energy values were then extracted and concatenated to form the two lowest-energy potential surfaces. In this way, the two lowest energy states could always be determined, even if the relative energies of the SCF orbitals changed in different parts of configuration space. As this system is open-shelled, unrestricted SCF and MP2 methods were employed exclusively.

Each of the potential surfaces was also corrected for basis set superposition error (BSSE) by employing the full counterpoise method [26]. In general, the BSSE corrections were less than 1% over much of the configuration space explored. However, for intermediate radial distances, these corrections were significant; in some cases, they affected the shape of the outer well in the approach to the asymptotic region. While this particular part of the potential surface is not very important for the present mobility calculations (which depend primarily on the position and anisotropy of the repulsive wall) it is important for calculations of spectroscopic parameters.

The potential surfaces were calculated in Jacobi coordinates whose origin lay at the center of mass of the H_2O^+ ion. The internal coordinates of the ion are held fixed at the calculated equilibrium geometry [24] with an OH bond length of 0.9980 Å, and an HOH bond angle of 109.57°. The plane of the ion was coincident

with the *yz* plane, with the oxygen atom lying on the negative *z*-axis. The *x*-axis was thus perpendicular to the plane of the ion. The helium atom was located by a set of triples (R, θ, α), where **R** was the vector from the origin to the helium atom, θ was the angle between the *z*-axis and **R** ($\cos\theta = \hat{\mathbf{R}} \cdot \hat{\mathbf{z}}$), and α was the angle between the *x*-axis and the projection of **R** in the *xy* plane. This triple corresponds with the usual definition of spherical polar coordinates. Thus, $\theta = 0$ and $\theta = 180°$ specify directions coincident with the C_2 axis of H_2O^+ with approach toward the hydrogen side and oxygen side, respectively, of the ion. All four atoms are coplanar when $\alpha = 90°$, and the helium lies perpendicular to the H_2O^+ plane when $\alpha = 0$.

Because of the C_{2v} symmetry of H_2O^+, only one-quarter of the entire configuration space needs to be mapped, with the remaining three-quarters determined from symmetry. Single-point energies were calculated at a series of points specified by R from 1.15–2.45 Å in steps of 0.05 Å, 2.5–3.9 Å in steps of 0.1 Å, 4.0–5.0 Å in steps of 0.25 Å, 5.5 Å, 6–11 Å in steps of 1 Å; by θ from 0°–180° in steps of 12°; and by α from 0°–90° in steps of 10° for a total of 8,640 points.

The calculated values of the both the ground and first-excited states are available in electronic form as part of the supplementary material associated with this manuscript.

Ion mobilities were calculated using a classical molecular dynamics algorithm described in Ref. [27], generalized to nonlinear ions. This algorithm requires radial and angular derivatives of the ground state potential energy surface. These were obtained by fitting the ab initio points to a three-dimensional cubic spline (using the MatLab software suite) [28] and then determining derivative values on fine, uniform grids from the spline expressions. These finer grids of derivative values were then used as input for the molecular dynamics code.

3. Results

One slice through the two potential energy surfaces is shown in Figure 1 as a function of R and θ for $\alpha = 10°$. This corresponds to positions in which the helium atom is circling H_2O^+ in a plane that is just tilted slightly off from the direction normal to the plane containing the ion. The curve crossing is readily apparent at approximately $R = 1.4$ *Å* for $\theta = 180°$. A crossing exists at similar radial distances for $\theta = 0°$, but is hidden behind the upper surface due to the perspective of the figure. The crossing occurs

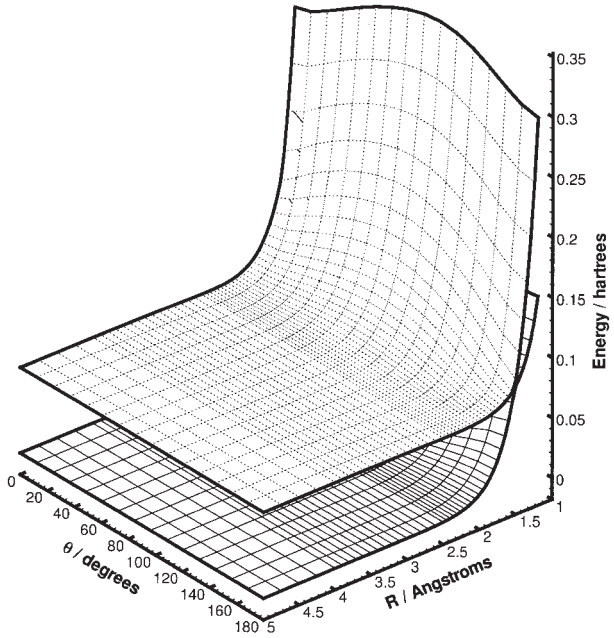

FIGURE 1. Plots of the ground and first-excited states of the H_2O^+–He complex as a function of θ and R with $\alpha = 10°$. The curve crossing is apparent at $\theta = 180°$. A similar crossing is also present for $\theta = 0°$ but is not visible in the plot.

only when the helium atom is coplanar with the ion, that is, $\alpha = 90°$, so that all the crossing points taken together form a closed curve in this plane around H_2O^+. The origin of this crossing is accidental, as outlined below, and is not mandated by symmetry arguments.

When the helium atom lies along the *z*-axis, that is, $\theta = 0°$ or $\theta = 180°$, the entire system has C_{2v} symmetry. For this arrangement, at asymptotically large distances, the orbital configurations of the ground and excited states are $(A_1)^2(A_1)^2(B_2)^2(B_1)(A_1)^2(A_1)^2$ and $(A_1)^2(A_1)^2(B_2)^2(A_1)^2(B_1)^2(A_1)$, respectively, so that the ground state has $^2B_1$ symmetry and the excited state $^2A_1$ symmetry. The molecular orbital of B_1 symmetry corresponds roughly to the lone-pair orbital on the oxygen atom, and has its major component from the p_x orbital on oxygen. The highest lying orbital of A_1 symmetry is a bonding orbital formed mainly from the overlap of the p_z orbital on oxygen with the *s* orbitals on each hydrogen. Thus, at large distances and compared with the electronic structure for water, the ground state of H_2O^+ corresponds to the removal of one electron from the lone-pair orbital on oxygen, while the first-excited state corresponds with removal of one electron

from the bonding orbital. At these distances, the $^2B_1$ state is lower in energy than the $^2A_1$ state.

When the helium is moved to closer distances, its *s* orbitals mix with the highest energy A_1 orbitals and cause their energy to rise. This effect is greatest for the $^2B_1$ state, with the result that at small distances the $^2B_1$ state has an energy greater than the $^2A_1$ state. It has now become the first-excited state. Because these states are of different symmetry, they must cross at some radial distance. This is the crossing depicted in Figure 1. This crossing is accidental because it is not mandated by symmetry arguments; but rather arises from the change in relative energies of two electronic configurations.

When the helium atom is coplanar with the ion ($\alpha = 90°$) but is not along the *z*-axis, the system has C_s symmetry. For this arrangement, at asymptotically large distances, the orbital configurations of the ground and excited states are $(A')^2(A')^2(A')^2(A'')(A')^2(A')^2$ and $(A')^2(A')^2(A')^2(A')^2(A')^2(A'')^2(A')$, respectively, so that the ground state has $^2A''$ symmetry and the excited state $^2A'$ symmetry. The situation is analogous to that in the C_{2v} arrangement, with the A'' orbital corresponding to the lone-pair orbital on the oxygen, and the highest energy A' orbital to the bonding molecular orbital. Again, the relative energies of these states interchanges on moving to small radial distances, and since they are of different symmetries, a crossing occurs.

When the helium atom lies in a plane perpendicular to the plane of the ion ($\alpha = 0°$), the system also has C_s symmetry. However, the two lowest energy states are both of $^2A'$ symmetry because the symmetries of the highest lying orbitals change, as compared with the case when $\alpha = 90°$. On moving the helium atom to small distances, the relative ordering of the energy levels still occurs, but now these orbitals are allowed to mix with each other. The result is that no crossing occurs. Rather, the potential surfaces exhibit an avoided crossing structure.

For all other configurations, the system has no symmetry, so that all the orbitals belong to the C_1 group. At large radial distances, it is still possible to assign meaning to the various orbitals, and identify for instance, the lone-pair and bonding molecular orbitals. However, unlike the other arrangements discussed above, the two states are both of the same symmetry. On moving to smaller radial distances, all the orbitals are allowed to mix, producing an avoided crossing structure.

To summarize, the two surfaces cross only when the helium is coplanar with the ion. This crossing appears as a closed curve surrounding the ion in this plane. For noncoplanar geometries, the two surfaces do not cross but instead have an avoided-crossing structure, like that seen in Figure 1 when θ is different from 0° or 180°.

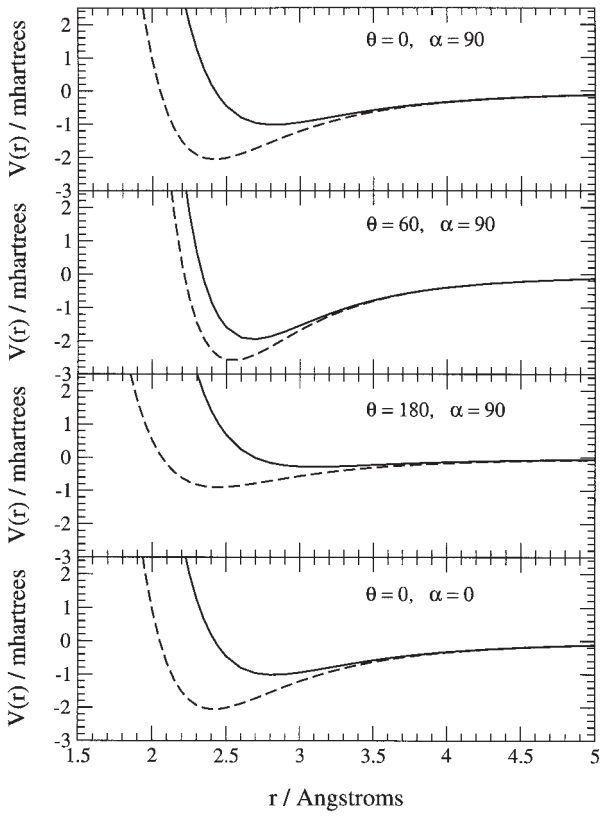

FIGURE 2. Radial plots at a few selected angles (given in each panel) of the H_2O^+–He complex. In each panel, the solid and dashed lines represent the ground and excited states, respectively. The excited state has been plotted with the same asymptote as the ground state for ease of visualization. In actual fact, the excited state lies ~71.4 mhartrees above the ground state.

A number of radial plots of the two surfaces at specific angles are shown in Figure 2. Note that the excited state surface has been plotted with the same asymptote as the ground state, even though this state lies ~71.4 mhartrees above the ground state. This was done in order to facilitate visual comparisons of the well regions. The top three panels in Figure 2 show the interactions when the helium is coplanar with the ion, and the bottom panel when it lies in a plane perpendicular to the ion. In each case, the excited state has a deeper well, and this well is shifted to smaller distances compared with the

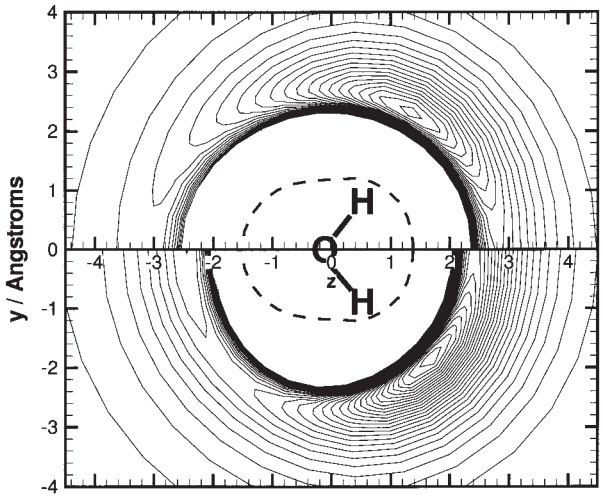

FIGURE 3. Contour plots for $\alpha = 90°$, that is, when helium is coplanar with H_2O^+. The upper and lower panels represent the ground and first-excited states, respectively. Contours are spaced at 0.1-mhartree intervals. The positions of the oxygen and hydrogen nuclei are represented by their chemical symbols. The dashed curve gives the location of the crossing between the two surfaces.

ground state. It is this shift which causes the two surfaces to cross high on the repulsive wall.

Figures 3 and 4 show contours of the surfaces for different planar cuts. The symmetry of the system, whereby only half of the plane is unique, was used to advantage by plotting the ground and excited state information on the same graph. The upper and lower halves of each plane correspond to the ground and excited states, respectively. Also, the position of the nuclei of H_2O^+ are also shown on the plots.

Figure 3 shows the contours when helium is coplanar with the ion (in the yz plane), that is $\alpha = 90°$. The ground-state surface has one minimum, the global one, located at $\theta = 60°$ and $R = 2.70$ *Å* with a well depth of 2.0 mhartrees. This minimum corresponds to an H-bound structure whereby the helium lies next to one hydrogen approximately along the OH bond direction. This hydrogen bonding structure agrees with that reported by Roth et al. [24], who report a global minimum with a well depth of 1.94 mhartrees located at $\theta = 59°$ and $R = 2.70$ *Å*.

The excited state surface also has a global minimum with a hydrogen bonding structure located at $\theta = 48°$ and $R = 2.50$ *Å* with a well depth of 2.8 mhartrees, but it also has a shallower well at $\theta = 180°$ along the negative z-axis. This latter minimum corresponds to an O-bound structure that is not present in the ground state. This well has a depth of 0.9 mhartrees; it is separated form the global minimum by a barrier of height 0.14 mhartrees located at $\theta = 133°$ and $R = 2.64$ *Å*. As shown in Figure 2, one can also see in Figure 3 that the excited state is contracted relative to the ground state when the system is coplanar.

Also shown in Figure 3 by a dashed line is the curve formed by the crossing of the two surfaces. This curve encircles the ion at small radial distances since the crossing occurs high on the repulsive wall.

As pointed out by Roth et al. [24], the two equivalent H-bonding structures are separated by a transition state located at the minimum along the z-axis. Hindered rotation of the ion through this transition state then interconverts one H-bonded structure into the other. For the ground state, the barrier to this interconversion is about 0.9 mhartrees, and for the first-excited state, it is roughly the same at 0.8 mhartrees.

Contours are shown in Figure 4 when the helium moves in a plane perpendicular to the ion (the xz plane), that is, when $\alpha = 0°$. The ground-state surface shows a shallow well of 1.0 mhartree located at $\theta = 0°$ and $R = 2.81$ *Å*. In the ground state, the helium has an affinity for the hydrogen side of the

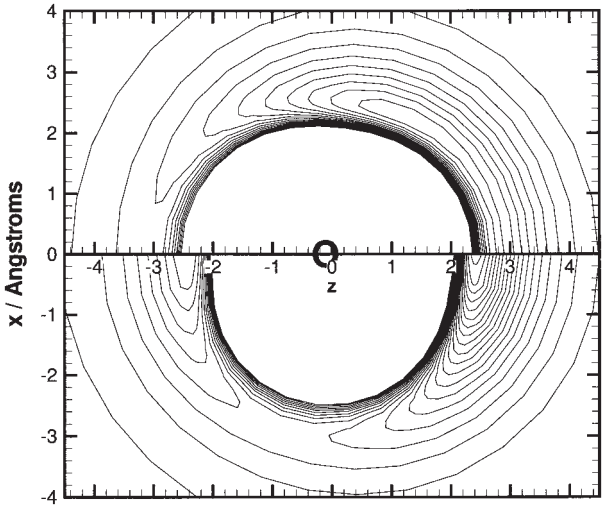

FIGURE 4. Contour plots for $\alpha = 0°$, that is when helium lies in a plane normal to the ion. The upper and lower panels represent the ground and first-excited states, respectively. Contours are spaced at 0.1-mhartree intervals. The position of the oxygen nuclei is represented by its chemical symbol.

ion compared with the oxygen side. However, this affinity is not very great, and large-amplitude motion can occur in this perpendicular plane quite readily. Roth et al. [24] reported a minimum when $\alpha = 0°$ located at $\theta = 100°$ and $R = 2.57$ *Å* corresponding to a *p*-bound structure. This minimum is not present in Figure 4 because the present calculation uses a rigid ion approximation. Roth et al. [24] employed a gradient optimization method with relaxation of the ion internal coordinates in order to locate this minimum. Thus, relaxation of the ion structure is necessary for this minimum to appear. The values of the fixed ion used here displace the system away from this minimum.

In contrast, the first-excited state has wells located at both $\theta = 0°$ and $\theta = 180°$ of depths 2.1 and 0.9 mhartrees, and radial distances of 2.41 and 2.44 Å, respectively. These two wells are separated by a barrier located at $\theta = 106°$ and $R = 3.02$ *Å* of height 0.64 mhartrees above the shallower well. Compared with the ground state, the excited state binds the helium more strongly, and also shows two stable isomers with the helium bound at both the hydrogen and oxygen end of the ion in O-bound and bridge structures. Large-amplitude motion in this plane is not easily induced on the excited state surface. Again, the excited state surface is contracted compared with the ground state, as evidenced by the shift of the wells and repulsive wall to shorter distances.

Overall, considering the full dimensionality of the surfaces, the ground state surface has a topology that always attracts the helium atom to the global minimum, that is the hydrogen-bonded geometry. The first-excited state surface, in contrast, attracts the helium to this same H-bound structure, but only when the helium is near the hydrogen end of the ion. If the helium is near the oxygen end of the ion, it is attracted to the O-bound structure associated with the minimum along the negative *z*-axis.

The results of mobility calculations using these global surfaces are shown in Figure 5. For the reduced field strengths employed here, the surface crossing seen in Figure 1 is located at an energy which is an order of magnitude greater than the average collision energy in the system. For this reason, only the ground state surface needs to be employed, and explicit treatment of the crossing can be ignored. This is fortunate, as such a treatment would be beyond the purely classical approach used in the molecular dynamics code. Comparison of the calculated and experimental

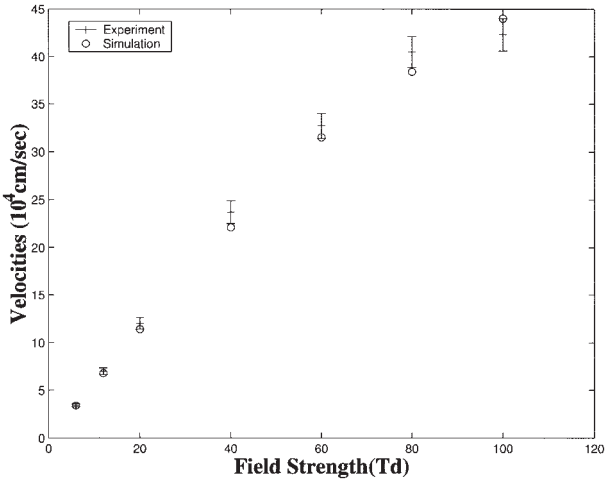

FIGURE 5. Comparison of calculated drift velocities for H_2O^+–He with measurements taken from Ref. [29] at a series of reduced field strengths.

mobilities in Figure 5 shows excellent agreement. This implies that the potential surfaces are of good quality, especially for mobility calculations.

4. Conclusions

Global potential energy surfaces for the ground and first-excited states of helium interacting with a rigid H_2O^+ ion are presented. The ground-state surface has a global minimum at the hydrogen-bonded geometry wherein the helium atom lies along approximately the OH bond direction, at a distance just beyond the hydrogen when all the atoms are coplanar. The topology of the ground surface always directs the helium atom to this global minimum. In contrast, the excited state surface also has a global minimum at this hydrogen-bonded geometry; however, the bond is shorter and stronger than that of the ground state. In addition, the excited state surface also has another stable configuration with the helium located beside the oxygen of the ion along the C_{2v} axis. The well depth at this configuration is shallower than that in the hydrogen-bonded configuration. Overall, the excited state surface is contracted compared with the ground state, with its wells and repulsive wall shifted to smaller radial distances.

The object of the present work was to produce a surface that would be capable of predicting gas-phase ion mobilities. The surfaces calculated in the present case proved to be of good quality as pre-

dictions of mobilities agreed very well with experimental measurements. These surfaces can now be employed for more detailed studies, like those of collision-induced alignment, for this system.

ACKNOWLEDGMENTS

The authors are especially grateful to Dr. Hopfer for providing the input data for the basis set.

References

1. Hoaglund-Hyzer, C. S.; Clemmer, D. E. Anal Chem 2001, 73, 177.
2. Srebalus Barnes, C. A.; Clemmer, D. E. Anal Chem 2001, 73, 424.
3. Valentine, S. J.; Counterman, A. E.; Clemmer, D. E. J Am Soc Mass Spectrom 1999, 10, 1188.
4. von Helden, G.; Wyttenbach, T.; Bowers, M. T. Science 1995, 267, 1483.
5. Gidden, J.; Wyttenbach, T.; Batka, J. J.; Weis, P.; Jackson, A. T.; Scrivens, J. H.; Bowers, M. T. J Am Soc Mass Spectrom 1999, 10, 883.
6. Harich, S.; Wodtke, A. M. J Chem Phys 1997, 107, 5983.
7. Aquilanti, V.; Ascenzi, D.; Cappelletti, D.; Fedeli, R.; Pirani, F. J Phys Chem A 1997, 101, 7648.
8. Aquilanti, V.; Ascenzi, D.; Cappelletti, D.; de Castro, M.; Pirani, F. J Chem Phys 1998, 109, 3898.
9. Anthony, E. B.; Bastian, M. J.; Bierbaum, V. M.; Leone, S. R. J Chem Phys 2000, 112, 10269.
10. Anthony, E. B.; Bierbaum, V. M.; Leone, S. R. J Chem Phys 2001, 114, 6654.
11. Meyer, H.; Leone, S. R. Mol Phys 1988, 63, 705.
12. Follmeg, B.; Rosmus, P.; Werner, H.-J. J Chem Phys 1990, 93, 4687.
13. Follmeg, B.; Werner, H.-J.; Rosmus, P. J Chem Phys 1991, 95, 979.
14. Aquilanti, V.; Ascenzi, D.; Vitores, M. D.; Pirani, F.; Cappelletti, D. J Chem Phys 1999, 111, 2620.
15. Fair, J. R.; Nesbitt, D. J. J Chem Phys 1999, 111, 6821.
16. Baranowski, R.; Thachuk, M. J Chem Phys 1999, 111, 10061.
17. Baranowski, R.; Wagner, B.; Thachuk, M. J Chem Phys 2001, 114, 6662.
18. Baranowski, R.; Thachuk, M. Phys Rev A: At Mol Opt Phys 2001, 63, 032503.
19. Baranowski, R.; Thachuk, M. Phys Rev A: At Mol Opt Phys 2001, 64, 062713.
20. Chen, Xin; Araghi, R.; Baranowski, R.; Thachuk, M. J Chem Phys 2002, 116, 6605.
21. Dopfer, O. J Phys Chem A 2000, 104, 11693.
22. Dopfer, O.; Roth, D.; Maier, J. P. J Phys Chem A 2000, 104, 11702.
23. Dopfer, O.; Roth, D.; Maier, J. P. J Chem Phys 2001, 114, 7081.
24. Roth, D.; Dopfer, O.; Maier, J. P. Phys Chem Chem Phys 2001, 3, 2400.
25. Frisch, M. J.; Trucks, G. W.; Schlegel, H. B.; Scuseria, G. E.; Robb, M. A.; Cheeseman, J. R.; Zakrzewski, V. G.; Montgomery Jr., J. A.; Stratmann, R. E.; Burant, J. C.; Dapprich, S.; Millam, J. M.; Daniels, A. D.; Kudin, K. N.; Strain, M. C.; Farkas, O.; Tomasi, J.; Barone, V.; Cossi, M.; Cammi, R.; Mennucci, B.; Pomelli, C.; Adamo, C.; Clifford, S.; Ochterski, J.; Petersson, G. A.; Ayala, P. Y.; Cui, Q.; Morokuma, K.; Rega, N.; Salvador, P.; Dannenberg, J. J.; Malick, D. K.; Rabuck, A. D.; Raghavachari, K.; Foresman, J. B.; Cioslowski, J.; Ortiz, J. V.; Baboul, A. G.; Stefanov, B. B.; Liu, G.; Liashenko, A.; Piskorz, P.; Komaromi, I.; Gomperts, R.; Martin, R. L.; Fox, D. J.; Keith, T.; Al-Laham, M. A.; Peng, C. Y.; Nanayakkara, A.; Challacombe, M.; Gill, P. M. W.; Johnson, B.; Chen, W.; Wong, M. W.; Andres, J. L.; Gonzalez, C.; Head-Gordon, M.; Replogle, E. S.; Pople, J. A. Gaussian 98, Revision A.11.4, Gaussian: Pittsburgh PA, 2002.
26. Boys, S. F.; Bernardi, F. Mol Phys 1970, 19, 553.
27. Baranowski, R.; Thachuk, M. J Chem Phys 1999, 110, 11383.
28. Spline Toolbox For Use with Matlab, User's Guide, Version 3.0; 2003 (http://www.mathworks.com).
29. Ellis, H. W.; Pai, R. Y.; Mcdaniel, E. W.; Viehland, A. L.; Mason, E. A. Atomic Data and Nuclear Data Tables 1976, 17, 177.